Available online at www.sciencedirect.com

ScienceDirect

Procedia Technology 26 (2016) 245 – 251

Procedia Technology

3rd International Conference on System-integrated Intelligence: New Challenges for Product and Production Engineering, SysInt 2016

Novel design concept of an optoelectronic integrated RF communication module

Quang Huy Dao[a,*], Alexandra Skubacz-Feucht[b], Bernard Lüers[a], Philipp von Witzendorff[c], Christoph von der Ahe[b], Ludger Overmeyer[b], Bernd Geck[a]

[a]*Institute of Radiofrequency and Microwave Engineering, Leibniz Universität Hannover, Appelstraße 9a, 30167 Hannover, Germany*
[b]*Institute of Transport and Automation Technology, Leibniz Universität Hannover, An der Universität 2, 30823 Garbsen, Germany*
[c]*Laser Zentrum Hannover e.V., Hollerithallee 8, 30419 Hannover, Germany*

Abstract

This contribution presents a novel design concept of a 24 GHz radio frequency communication module. The integration of optical and electrical components is a particular challenge since the module is miniaturized in order to be integrated into any metallic workpieces. The design concept and the scope of functions of the communication unit acting as a wireless sensor node are discussed. The development of a highly integrated radio frequency circuit and the realization of through glass vias are some main aspects. The central control unit is an ultra-low power microcontroller capable of a flexible connection of sensors. By using an energy harvesting concept consisting of a solar cell with an efficiency of 40 % and a supercapacitor the availability of energy is unlimited. Different lighting conditions are investigated in order to evaluate the available power of the solar cell. Furthermore, the power supply is investigated concerning voltage-current characteristics and the resulting operating time of the whole unit for a low ambient light scenario.

Peer-review under responsibility of the organizing committee of SysInt 2016

Keywords: 24 GHz RFID; wireless sensor node; RF communication; 3D-MID; optoelectronic packaging; optical power transfer

* Corresponding author. Tel.: +49 511 762 4112; fax: +49 511 762 4010.
E-mail address: dao@hft.uni-hannover.de

Peer-review under responsibility of the organizing committee of SysInt 2016
doi:10.1016/j.protcy.2016.08.033

1. Introduction

Due to increasing markets, requirements such as product quality, a high flexibility, functional range and availability are essential to succeed within international competition. Especially as product lifecycles get shorter and manufacturing changes for individualized products from mass goods down to batch size one. This tendency leads to a vast variety of products and a large number of possible processes and process chains.

In order to find the optimal solution, e.g. the fastest lead-time and best design, new approaches for adaptive manufacturing planning, the monitoring of production steps and online process-monitoring during the product lifecycle are needed [1]. Therefore, each component has to be clearly identifiable and locatable. In this context, product intelligence and cyber-physical systems (CPS) play an important role. For self-organizing processes and autonomous productions the necessity to give up the physical separation between components and its related information is essential. By using the proposed wireless communication module which will be presented in next section all relevant data e.g. design and process parameters, load information, are available on the device and enable a closed information loop over the lifecycle of the workpiece [2]. The data gathered from integrated sensor systems can be transmitted at any time to a reading/writing unit for analysis in order to improve the manufacturing process in an efficient way. In addition to that, relevant information can be used to enhance the product quality.

Against this background, a novel design concept of an optoelectronic integrated RF communication module for the integration into metallic components is presented. The wireless communication is based on the Radio Frequency Identification (RFID) principle [3] and operates in the 24 GHz industrial scientific and medical (ISM) radio band. Thereby, a high data transmission and reduced latency time is enabled. Due to the optical power supply concept with a highly efficient multijunction solar cell, the system functionality is ensured during the whole product lifecycle without requiring any batteries. The small mounting volume (13 x 13 x 4 mm³) of the investigated communication module is interesting for many applications and especially for the integration into load bearing metallic objects.

2. Design concept

The novel design concept of the RF communication module, which can be integrated into the head of the screw is depicted in Fig. 1. The exploded view shows the highly integrated multi-layer structure with the fusion of electronical and optical components. This module consists of four main parts. First of all, a housing is needed to carry the individual layers. A promising approach is the use of three dimensional molded interconnect devices (3D-MID) acting as circuit carriers [4]. By means of the laser direct structuring (LDS) process electronic conducting paths can be created directly on the plastic compounds. In this way it is possible to design any 3D circuits by using the third dimension in an

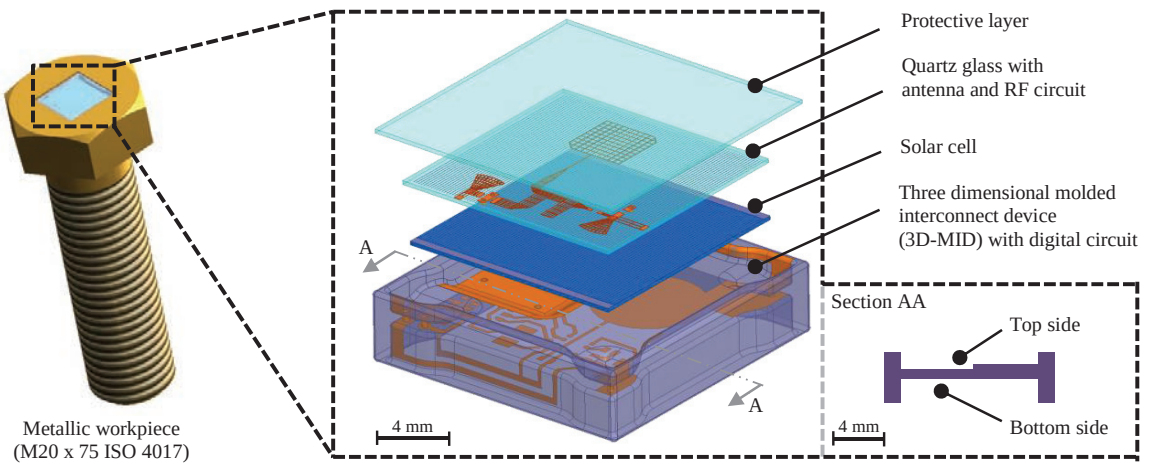

Fig. 1. 24 GHz communication module integrated into a metallic workpiece; exploded view of the module and cross section view of the 3D device

efficient way. In the presented case the bottom and the top side of the housing including the inner walls are used to realize the conductor tracks for the electrical connection of the solar cell and the RF circuit. The proposed housing has a volume of 13 x 13 x 4 mm³. On the bottom side of this housing space is available for the integration of a digital circuit consisting of an ultra-low power microcontroller and an energy storage. In order to enable a continuous process monitoring of load parameters such as temperature or strain, it is possible to add additional sensor systems to the microcontroller. To connect the digital circuit with the top layer through hole vias are used. This production step can be realized completely within the LDS process. Hereby, the laser drills through the plastic compounds and at the subsequent metallization process copper deposits in the hole. In this way, a reliable connection can be achieved.

The main part of the energy harvesting concept is the solar cell which is placed on the 3D-MID component. Since wire bonding is more prone to damage by vibrations the electric interconnection of the solar cell with the digital and RF circuit is achieved by conductive adhesives. Therefore, the entire back panel area of the solar cell providing the positive voltage is fully adhered to the top side of the 3D-MID component. Hence, a reliable mechanical connection is realized. The interconnection between the front-side (ground connections) of the solar cell, so called busbars, and the conductor tracks on the side walls of the 3D-MID is also done by conductive adhesive. It is still to be determined whether a reactive or non-reactive adhesive should be used, depending on which type of adhesive suits the requirements best. To avoid short-circuits throughout the bonding process isolation has to be fitted between the two terminals of the solar cell. This isolating layer can consists of a non-conductive adhesive.

The RF circuit including an antenna is arranged on the solar cell. A promising approach of the antenna concept is the use of a patch antenna. Moreover, the patch antenna structure can be designed as thin grid lines made of conventional metal in order to achieve optical transparency [5]. The RF circuit can be realized in the same way to minimize the shading effects caused by strip lines. Furthermore, by designing the antenna and the analog frontend on the same layer attenuation losses due to electrical connections between separated layers can be reduced. Quartz glass is preferred as carrier substrate for these structures since it has a high optical transparency. An additional reason is the low dissipation factor of the material concerning electromagnetic properties (see section 3.1).

To protect the communication module against environmental influences such as dust, dirt, lubricants, metal chips, etc. a protective layer made of quartz glass plate is provided. This layer should fulfill requirements such as high optical transparency and resistance against environmental impact. Thus, it is possible to adapt the surface conditions through specific surface treatments.

3. Communication module

The wireless communication between the reading/writing unit and the presented module is based on the radio frequency identification (RFID) principle. A block diagram of the used RFID system is depicted in Fig. 2. The reader/writer is shown on the left hand side while the communication module/transponder is illustrated on the right hand side. The data transmission process from the transponder to the reader/writer e.g. transmission of the actual

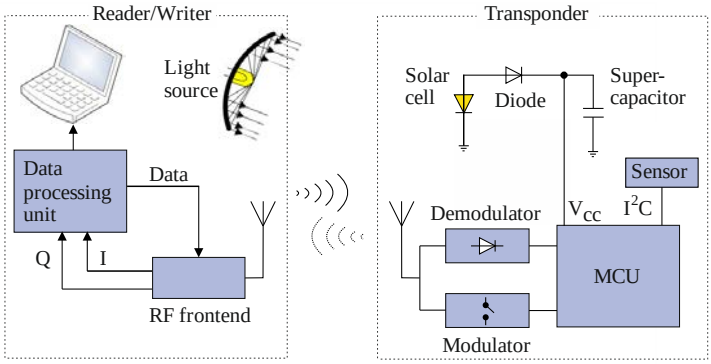

Fig. 2. Block diagram of the RFID system

temperature value can be described as follows: The reader/writer transmits a request to the transponder via the RF frontend. In this case amplitude shift keying (ASK) modulation is accomplished by a PIN diode switch which is controlled by the data processing unit. Hereby, the carrier frequency is 24 GHz. The request signal is demodulated by an analog frontend of the transponder. By using a microcontroller (MCU) the command can be interpreted and a response can be generated utilizing the modulator unit. The backscattered transponder signal is converted into the baseband and this signal is routed through the inphase (I) and quadrature (Q) channel to the data processing unit of the reader/writer. Afterwards, the actual temperature value of the transponder is displayed on a computer.

To power the MCU an energy harvesting concept consisting of a high efficient solar cell and a supercapacitor acting as energy storage is used. Thus, an external light source such as a halogen lamp or sufficient ambient light is necessary in order to supply electrical power to the transponder. Thanks to the I²C bus of the MCU additional sensors such as acceleration sensors can be easily integrated within the transponder to expand its scope of functions. The preferred ultra-low power microcontroller is a MSP430FR5738 from Texas Instrument. It requires at least 1.97 V for a proper operation and the current consumption varies between 37 µA and 800 µA depending on the actual operating state. An additional advantage of this microcontroller is the integrated 16 kB non-volatile memory sufficient for storage information such as production data and load parameters during the life time of a workpiece.

3.1. Modulator and demodulator

In this section the analog frontend of the communication module will be presented in detail. The layout of the realized modulator and demodulator circuit is illustrated in Fig. 3. This circuit is arranged at the feed point of the antenna (c.f. Fig. 1). Similar circuit topology was shown and well described in previous publications [2], [6] but the structures were realized on conventional opaque laminate. To evaluate the functionality of the proposed analog frontend quartz glass is used as carrier material since it has a high optical transparency. For the first evaluation and testing purposes the microstrip lines do not consist of grid lines as shown in Fig. 1. Thus, the optical transparency of the strip lines is initially zero in this investigation. The permittivity $\epsilon_r' = 3.81$ and the loss angle $\tan\delta = 0.0004$ of the quartz glass are measured by the resonator method at the frequency of 24 GHz. The whole circuit is designed and optimized using the simulation software Advanced Design Systems 2009.

The envelope demodulator consists of a zero bias GaAs Schottky diode (Keysight HSCH-9161) and a 0.3 pF capacitor. The modulator is based on an Avago VMMK-1225 High Electron Mobility Transistor (E-pHEMT) acting as a switch in a common source configuration. By applying a gate source voltage V_{GS} two different input reflection coefficients $\Gamma_{1,2}$ can be achieved. Hence, data can be transmitted to the reader/writer by changing the voltage level. Fig. 4a depicts the simulated and measured reflection coefficients of the modulator and demodulator. The matched case Γ_1 and the mismatched case Γ_2 are obtained for $V_{GS} = 0$ V and $V_{GS} = 0.7$ V, respectively. A good agreement for the matched case can be achieved concerning the position of the resonance frequency and for the mismatched case there is a difference of 0.4 dB at the frequency of 23.76 GHz. The output voltage envelope V_{out} of the demodulator for

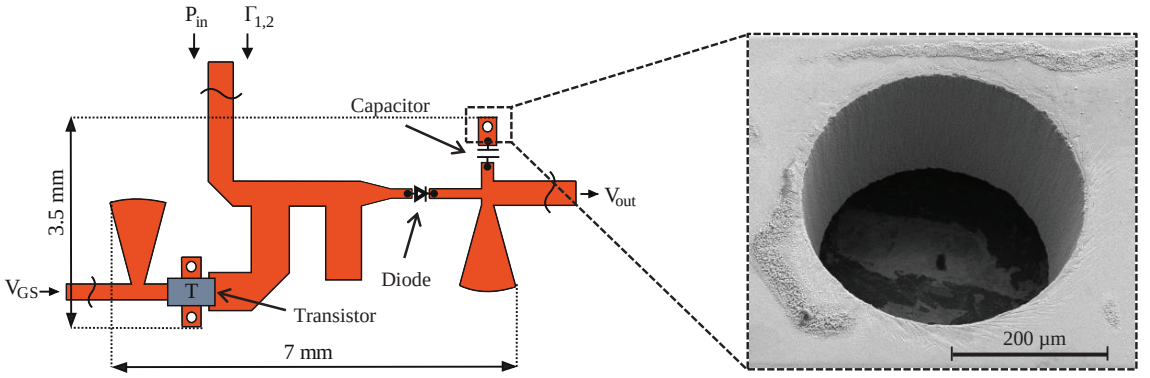

Fig. 3. Left: Layout of the realized modulator and demodulator circuit; right: SEM image of a through glass via

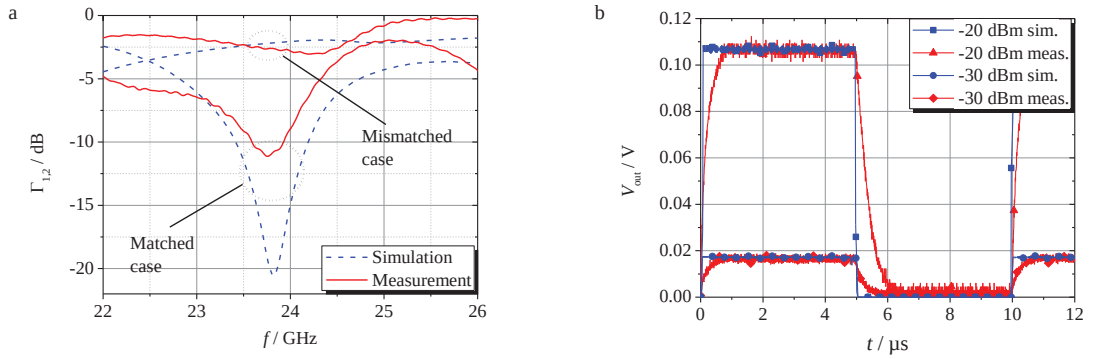

Fig. 4. Comparison between simulation and measurement results; (a) Reflection coefficients for two different states at an input power P_{in} of – 20 dBm; b) Voltage signal V_{out} at the output of the demodulator

two different input power P_{in} are shown in Fig. 4b. In this case an RF signal modulated with a 100 kHz square wave is used as input signal. A good agreement between simulation and measurement can be obtained. The mismatch concerning the slope of the envelope is caused by the measurement setup and mainly by the input capacitance of the oscilloscope.

In order to make the ground connections for the transistor and the capacitor, through glass vias are produced by laser ablation with a picosecond laser source with 515 nm wavelength. An example of a via is presented in Fig. 3. The laser radiation is deflected with a galvanometric scanning system to irradiate the drill hole. The average laser power is set to 3 W at 50 kHz pulse repetition rate. The focal spot size was 20 µm. After the production of the through glass vias, the glass substrate is RF sputtered with copper on both sides. In this way, an electrical connection can be obtained.

4. Optical power supply

The power supply concept of the communication module is based on a single metamorphic solar cell in combination with a supercapacitor acting as an energy storage (c.f. Fig. 2). The used multijunction III-V concentrator solar cell C4MJ produced by Spectrolab is a fully qualified triple junction GaInP/GaInAs/Ge solar cell [7-8]. According to the AM1.5D, ASTM G173-03 standard this solar cell reaches an efficiency of 40% at 500 suns (50 W/cm²) [9]. The solar

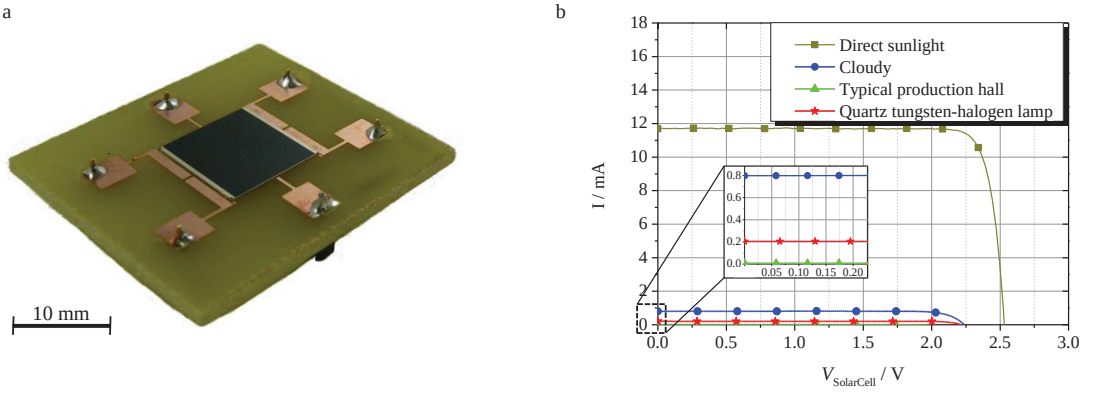

Fig. 5. (a) Picture of the used multijunction solar cell which is bonded on a FR4 substrate for characterisation; (b) Current-voltage characteristics for different lighting scenarios

cell which is bonded on a FR4 substrate for electrical characterization is depicted in Fig. 5a. The geometric dimensions of the optical aperture are 10 x 9.9 mm². The thickness is 0.2 mm. The busbars on the top side are the ground reference with a width of 0.4 mm while the whole bottom side provides the positive voltage. This mounting configuration is used for a characterization of current-voltage curves for different lighting scenarios. The measurement results obtained by a source measure unit Keysight B2900A are shown in Fig. 5b. By applying direct sunlight to the solar cell the short-circuit current I_{SC} is 11.7 mA while the open-circuit voltage V_{OC} is 2.52 V. On a cloudy day the solar cell delivers a current I_{SC} of 0.8 mA. In this case V_{OC} is 2.23 V. The performance of the cell is also evaluated in a typical production hall (Hannover Centre for Production Technology PZH) resulting in the curve marked with triangles. These values are averaged for five different positions within the production hall. The available ambient light provides a current I_{SC} of 9 µA and the voltage V_{OC} is 1.85 V, respectively. This indoor lighting is not sufficient to power the digital circuit since the microcontroller requires at least 1.91 V to function properly. Thus, an external quartz tungsten-halogen lamp can be used as an additional light source. The selected lamp Thorlabs QTH10/M including a condensing lens offers a broadband illumination in the visible and near-IR portions of the light spectrum (400 – 2400 nm) [10]. The quartz tungsten-halogen bulb requires 10 W at a DC voltage of 12 V. To obtain the current-voltage characteristic, this lamp is positioned at a distance of d = 2 m away from the solar cell since the communication distance between reader/writer and the transponder is in this range. For this measurement setup the current I_{SC} is 0.2 mA and the voltage V_{OC} is 2.21 V. This lighting condition is sufficient to power the whole communication module.

4.1. Energy storage and operating time of the transponder

The energy harvesting concept is designed in a manner that the energy out of the solar cell is buffered in an Elna DCK-3R3E204T614 supercapacitor with a capacitance of 0.2 F. A simple schematic is illustrated in Fig. 6a. A Schottky diode BAT30F4 from STMicroelctronics is used to minimize the discharging process of the capacitor during the low light environment. This diode is suitable for this application because of the low forward voltage drop and a reverse leakage current lower than approx. 1 µA at room temperature.

To evaluate the efficiency of the proposed energy harvesting concept different lighting conditions are tested. In the following, one fixed scenario is defined to find out the operating time of the transponder. In this scenario the halogen lamp QTH10/M is positioned at a distance d of 2 m (c.f. Fig. 6a). The energy is consumed by the microcontroller and the modulator during the experiment. At the beginning, the voltage of the capacitor V_{Cap} is 0.01 V (empty state). A source measure unit Keysight B2900A is utilized to capture the voltage of the capacitor and the current of the solar cell during the charging and discharging process of the energy storage. These curves are depicted in Fig. 6b. First of all, the lamp is switched on at a time of 60 seconds and the forward current of the diode changes to 0.22 mA. During the whole measurement the reading/writing unit transmitted a request for the actual temperature value of the transponder periodically (every second). When V_{Cap} reaches the voltage level of 1.97 V (t = 1364 s, at bright ambient

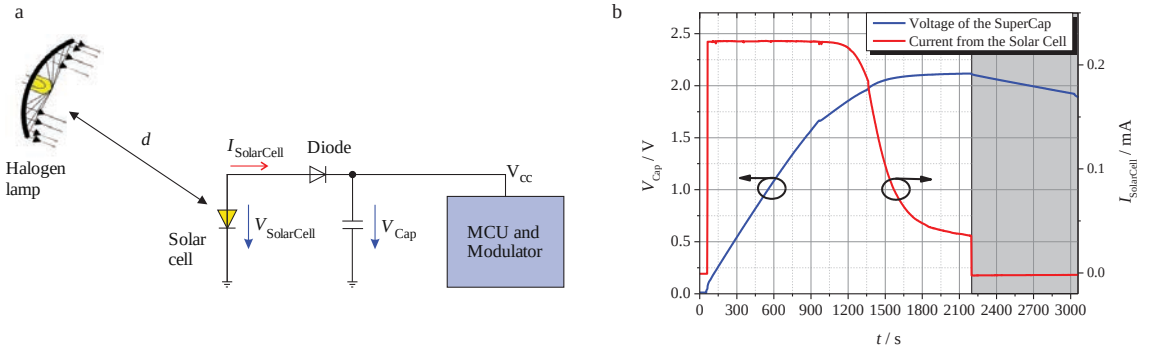

Fig. 6. (a) Schematic of the energy harvesting concept and setup for determining the operating time of the transponder; (b) Measured voltage V_{Cap} of the supercapacitor and current $I_{SolarCell}$ of the solar cell during the operating time of the transponder for a defined scenario.

light such as outdoor environment the threshold voltage will be reached in approx. two seconds) the microcontroller wakes up, processes the request, transmits a respond to the reader/writer and goes to sleep mode until the next incoming request. This communication procedure is repeated every second. From now on the current $I_{SolarCell}$ reduces until it reaches a current value of approx. 36 µA (t = 2196 s). This value is the average current consumption of the microcontroller. This means that within 36.6 min. the capacitor is fully charged and V_{Cap} is 2.11 V while the transponder is still transmitting data to the reading/writing unit periodically.

In the next step the halogen lamp is switched off to simulate the operating time of the transponder in a low ambient light. The greyed area in Fig. 6b illustrates the scenario of discharging the supercapacitor. During this period, the reverse leakage current of the diode varies between 1.3 and 0.9 µA. The voltage V_{Cap} decreases steadily. At the time of 3032 s, the voltage level of 1.91 V is not sufficient to power the microcontroller. In this case bidirectional communication cannot be maintained. For the investigated scenario it can be concluded that in a low ambient light the designed transponder can operate continuously for 13.9 minutes with a fully charged supercapacitor of 0.2 F while transmitting its actual temperature value every second.

4. Conclusion

This paper presents a design concept of a highly integrated radio frequency communication module operating at the 24 GHz ISM band. By using the three dimensional molded interconnect device (3D-MID) technology and the laser direct structuring (LDS) process, the fabrication of a housing acting as circuit carriers simultaneously can be realized. Thus, a compact size of the communication unit (13 x 13 x 4 mm³) is obtained. The developed analog frontend is investigated and a verification of the simulated results is done by measurement. A good agreement can be achieved. The central control unit is an ultra-low power microcontroller with an integrated non-volatile memory. Additional sensors can be added by the I²C bus to extend the scope of functions. Furthermore, the current-voltage characteristics of the utilized multijunction solar cell is determined under typical ambient light conditions. A supercapacitor stores the harvested energy and depending on its electric charge and voltage level the communication module can be powered even in case of complete darkness.

Acknowledgements

The authors wish to thank the German Research Foundation for the financial support in the framework of the Collaborative Research Center 653. Furthermore, the authors wish to thank Ms. Lisa Jogschies for her efforts in producing the structures on glass substrate.

References

[1] B. Denkena, T. Mörke, M. Krüger, J. Schmidt, H. Boujnah, J. Meyer, P. Gottwald,B. Spitschan, M. Winkens, Development and first applications of gentelligent components over their lifecycle, CIRP Journal of Manufacturing Science and Technology, Volume 7, Issue 2, 2014, p. 139-150.

[2] J. Meyer, Q. H. Dao, B. Geck, 24 GHz rfid communication system for product lifecycle applications, in 2nd International Conference on System-Integrated Intelligence: New Challenges for Product and Production Engineering (SysInt), 2014.

[3] K. Finkenzeller, RFID Handbook, 2nd ed. Wiley, 2004.

[4] J. Franke, Three-dimensional molded interconnect devices (3D-MID), Hanser, 2014.

[5] Q. H. Dao, T. J. Cherogony, B. Geck, Optically transparent and circularly polarized patch antenna for K-band applications, in 10th German Microwave Conference (GeMiC), 2016.

[6] J. Meyer, Q. H. Dao, B. Geck, Design of a 24 GHz analog frontend for an optically powered RFID transponder for the integration into metallic components, in 43nd European Microwave Conference (EuMC), 2013.

[7] Spectrolab, Datasheet C4MJ, Rev. 7/12/11. <http://www.spectrolab.com/DataSheets/PV/CPV/C4MJ_40_Percent_Solar_Cell.pdf>, 2016 (accessed 02.05.16).

[8] J. H. Ermer, R. K. Jones, P. Hebert, P. Pien, R. R. King, D. Bhusari, R. Brandt, O. Al-Taher, C. Fetzer, G. S. Kinsey, N. Karam, Status of C3MJ+ and C4Mj production concentrator solar cells at spectrolab, in IEEE Journal of Photovoltaics, Vol. 2, No. 2, 2012, p. 209-213.

[9] R. R. King, D. Bhusari, D. Larrabee, X.-Q. Liu, E. Rehder, K. Edmondson, H. Cotal, R. K. Jones, J. H. Ermer, C. M. Fetzer, D. C. Law, N. H. Karam, Solar cell generations over 40% efficiency, in Progress in Photovoltaics: Research and Applications, Vol. 20, Issue 6, 2012, p. 801-815.

[10] Thorlabs, User guide QTH10(/M) Quartz Tungsten-Halogen Lamp, Rev D, January 4, 2015, <http://www.thorlabs.de/newgrouppage9.cfm?objectgroup_id=7541&pn=QTH10/M>, 2016 (accessed 28.04.16).